·Synergistic strengthening behavior and microstructural optimization of hybrid reinforced titanium matrix composites during thermomechanical processing

Shaopeng Li [a], Yuanfei Han [a,b], Zhusheng Shi [c], Guangfa Huang [a], Nan Zong [a], Jianwen Le [a], Peikun Qiu [a], Weijie Lu [a,b**]*

[a] *State Key Laboratory of Metal Matrix Composites, School of Materials Science and Engineering, Shanghai Jiao Tong University, Shanghai, 200240, China*

[b] *Shanghai Key Laboratory of Advanced High Temperature Materials and Precision Forming, Shanghai 200240, China*

[c] *Department of Mechanical Engineering, Imperial College London, London SW7 2AZ, UK*

Abstract

In this study, titanium matrix composites (TMCs) reinforced with hybrid TiB, TiC and Re_xO_y (rare earth oxides) were successfully fabricated by vacuum arc melting technique. Subsequently thermomechanical processing was carried out to optimize the microstructure and investigate the synergistic strengthening behavior. It is found that the optimized microstructure mainly contained two typical regions: Region 1, reinforcement-lean region with coarse lamellar grains. Region 2, reinforcement-rich region containing fine equiaxed α grains comparing with reinforcement-lean region, all hybrid reinforcements distributed homogeneously at their grain boundaries and TiB fibers are perpendicular to the forging direction. It is shown that the reinforcement can stimulate the dynamic/static recrystallization during the thermomechanical processing. The tensile strength was significantly enhanced by the ternary reinforcements and the thermomechanical processing. A well-matched relationship between microstructure and mechanical properties is obtained. When the reinforcement content is 2.5 vol.%, the tensile strength at room temperature and high temperature (700 °C) increased to 1214 MPa and 552 MPa, while the TMCs maintained a good elongation of 5.1% and 58% respectively. The strengthening mechanism could be attributed to the refinement of the matrix grain, the solid solution strengthening of C element and the load-bearing capability of TiB and ternary oxide clusters.

Keywords: Titanium matrix composites, Thermomechanical processing, IMI834, Microstructure, Strengthening

*Corresponding author: Tel.: +86-21-34202641; Fax: +86-21-34202749

Email address: hyuf1@sjtu.edu.cn (Yuanfei Han); luweijie@sjtu.edu.cn (Weijie Lu)

1. Introduction

Titanium matrix composites (TMCs) reinforced with high strength and high stiffness ceramic particles/whiskers became one of the most potential materials in automotive and aerospace industries due to their superior properties, such as high specific strength, high specific stiffness, excellent wear resistance and favorable mechanical properties at elevated temperature [1,2].

To produce low-cost and high-performance TMCs, several processes have been developed as in-situ methods to fabricate TMCs, such as powder metallurgy (PM) [3-5], mechanical alloying (MA) [6], self-propagation high-temperature synthesis (SHS) [7,8], spark plasma sintering (SPS) [9,10] and ingot metallurgy technique (IM) [11,12]. Among these methods, vacuum consumable melting technology (one of IM) has made a rapidly development in recent years and is considered as a low-cost technology which can make the reinforcements evenly distributed in the matrix and achieve excellent interfacial bonding [13,14], and thus, it is widely used in the preparation of in-situ TMCs. However, IM still has problems of the coarse grain size and partial internal defects, which deteriorate the mechanical properties and limit broader application of TMCs.

Fortunately, several published works have shown that hot working and heat treatment can be used to tailor the microstructure and improve corresponding mechanical properties [15-19]. Up to now, the effect of conventional hot working include forging [15], extrusion [16,17], rolling [18], ECAP [19], etc on the TMCs have been investigated, which play a successful role in tailoring the microstructure and improving the strength and ductility. Among these hot working processes, forging is regarded as the most economical and convenient process, which significantly reduces casting defects and aligns discontinuous particles/whiskers perpendicular to the forging direction, further forming the reinforcement-rich and the reinforcement-lean region during the forging process. It can remarkably improve the strength, elastic modulus and ductility with both low or high reinforcement contents [20-22].

In earlier works, various reinforcements were proposed to enhance the comprehensive properties of TMCs, such as Ti_5Si_3, SiC, Al_2O_3, TiB, TiC, rare earth oxides, etc [23-30]. Among these candidates, TiB whiskers [23-25] and TiC particles [26,27] have been considered as the best reinforcements due to their good compatibility with matrix alloys, especially the similar density and the thermal expansion. Meanwhile, some researchers believe the addition of rare earth elements can react with oxygen by generating rare earth oxides, which can reduce oxygen content in matrix and

enhance the ductility [29]. Furthermore, nano-scale rare earth oxides, such as La_2O_3, Y_2O_3 and Nd_2O_3, etc., uniformly dispersed in matrix, play an important role in impeding dislocation motions to strengthen TMCs [30]. On this basis, the multi-phase and multi-scale design idea was proposed to further enhance the TMCs [31-33]. In recent years, several kinds of hybrid reinforced TMCs were designed to exert the synergistic strengthening effect. Yang and co-workers have carried out a lot of work on hybrid reinforced systems, such as (TiB+La_2O_3) [32], (TiB+TiC+Nd_2O_3) [34] and (TiB+TiC+La_2O_3) [35], mainly focusing on the high temperature properties. They found that the hybrid reinforcements significantly improve the mechanical properties, but the improvement decreases with the increase of temperature. Yang et al. [36] studied the as-cast (TiB+TiC+Y_2O_3)/α-Ti system, which achieved 160MPa increase on yield strength at room temperature, and found that the ternary reinforcement can refine the prior β grain. Qiu et al. [20] studied the as-extruded (TiB+TiC+La_2O_3)/TC4 system and found that the reinforcement stimulated the dynamic recrystallization during the extrusion process and the as-extruded TMCs exhibited a significant improvement on the ductility at low volume fraction of reinforcements. However, the above studies mainly focused on the as-cast and as-deformed TMCs, ignoring the optimization of the microstructural features to achieve the best performance, and few words are related to the synergistic strengthening mechanism, and the relationship among the reinforcement contents, microstructure and mechanical properties of TMCs with ternary reinforcement, especially for the as-forged and heat-treated TMCs.

In the present work, the IMI834 titanium matrix composites with different volume fraction of TiB, TiC and rare earth oxide were designed and fabricated by common casting. Subsequent hot forging and two-steps heat treatment were carried out to tailor the microstructure and enhance the tensile property. The microstructure evolution and mechanical properties of the heat-treated TMCs were investigated, especially focused on the synergistic strengthening effect and microstructural optimization mechanism of hybrid reinforcements during the whole thermomechanical processing.

2. Experimental procedures

2.1. Materials and Methods

IMI834 alloy was selected as the matrix alloy whose nominal composition is Ti-5.8Al-4.0Sn-3.5Zr-0.7Nb-0.5Mo-0.35Si-0.06C (wt.%). The raw materials were carbon powder (*d*

= 5-7μm), B_4C powder (d = 5-10μm), LaB_6 powder (d = 61-74μm), titanium sponge (wt.% ≥ 99.9%) and some intermediate alloy (wt.% ≥ 99.9%), where d is the diameter of the powders. Previous works provided a suitable range for each reinforcement [11,17,20,31,32]; (1) As for the total volume fraction, Qiu et al. [20] found that the strength can be greatly improved, while maintain a good ductility when the reinforcement content was limited below 2.5 vol.%. Considering the low ductility of the matrix alloy, the total volume fraction was set to 0.5, 2.5 and 5.0 vol.%. (2) As for the rare earth oxides, many studies have been concluded that the excessive addition of rare earth elements would cause the segregation and growth of rare earth oxides and greatly reduce the ductility, the good strengthening effect can be obtained when the rare earth oxide content is 0.29~0.58 vol.% [31,32]. (3) As for the ratio of TiB and TiC, Lu et al. [11,17] reported that (TiBw+TiCp)/Ti6242 composites possessed higher tensile strength and ductility with the TiB and TiC is 1:1. Thus, to obtain good comprehensive mechanical properties and investigate the synergistic strengthening effect of different reinforcement content, three billets were fabricated based on the summary of previous researches, the theoretical reinforcements contents are listed in table 1.

Table 1 Reinforcement content (vol.%) of (TiB+TiC+La_2O_3)/IM834 titanium matrix composites

Sample	TiB	TiC	La_2O_3	Total
TMCs 1	0.22	0.22	0.06	0.5
TMCs 2	1.1	1.1	0.3	2.5
TMCs 3	2.2	2.2	0.6	5.0

(TiB+TiC+La_2O_3)/IMI834 composites were in situ synthesized in the ZKY-10A non-consumable vacuum arc melting furnace. The reactions in this system are shown as follows:

$$Ti+C = TiC \quad (1)$$

$$5Ti+B_4C = 4TiB+TiC \quad (2)$$

$$12Ti+3[O]+2LaB_6 = 12TiB+La_2O_3 \quad (3)$$

Thermodynamic calculations provide a strong theoretical basis for the in-situ reactions, the results are shown in Fig. 1. It is obviously that both △G and △H of the in-situ reaction are negative, which indicates that these reactions are spontaneous exothermic reactions. Thus, it is thermodynamically feasible to synthesize reinforcement by the above reactions. To ensure the chemical composition and reinforcement homogeneity, each ingot was melted three times.

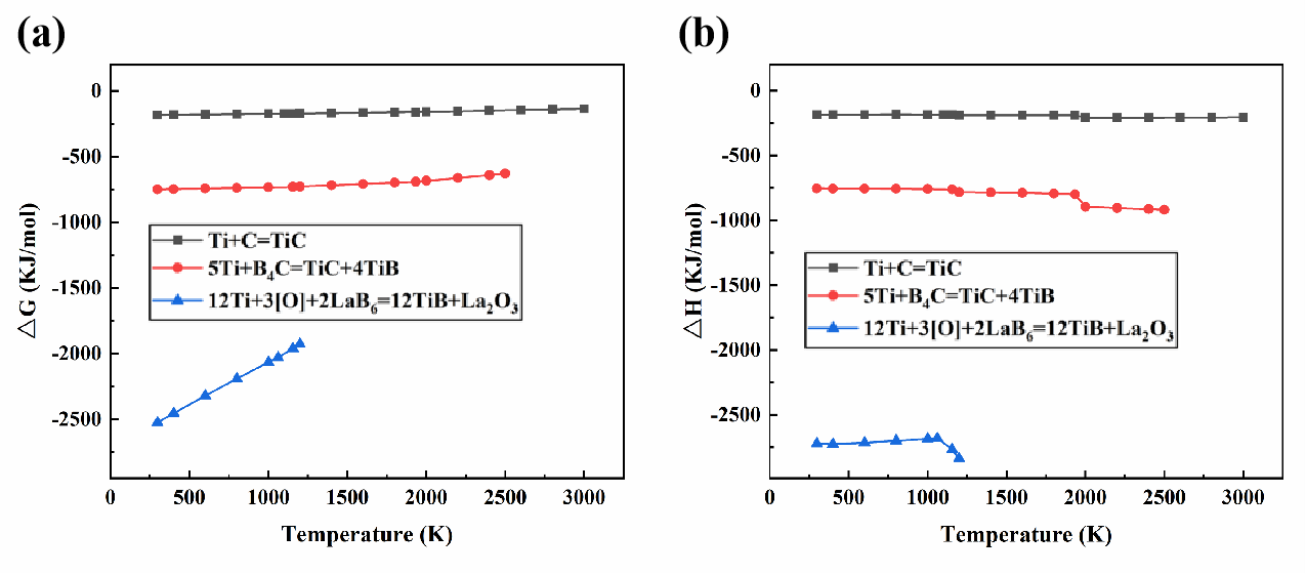

Fig. 1. Thermodynamic calculation of the in-situ reactions:

(a) Gibbs free energy, (b) Enthalpy change

2.2. Thermomechanical processing

Computational analysis method was used to calculate the phase transition temperature, considering the solid solution of alloying elements and different content of element C, the transition temperature (T_β) was identified as 1020-1040°C. Based on T_β, the hot working temperature was set at 980°C (α+β phase field). Fig. 2(a) shows the schematic of hot working process which includes:

- Hot deformation: each ingot was furnace heated and hold at 980°C for 1 hour, then forged in the α+β phase region with a deformation degree of 50% and subsequently air cooled to room temperature.
- HT 1: Recrystallization treatment process, the as-forged composites were heat treated at 1000°C for 1 hour and then air cooled to room temperature.
- HT 2: Ageing process, the billets were aged at 700°C for 2 hours and air cooled to room temperature.

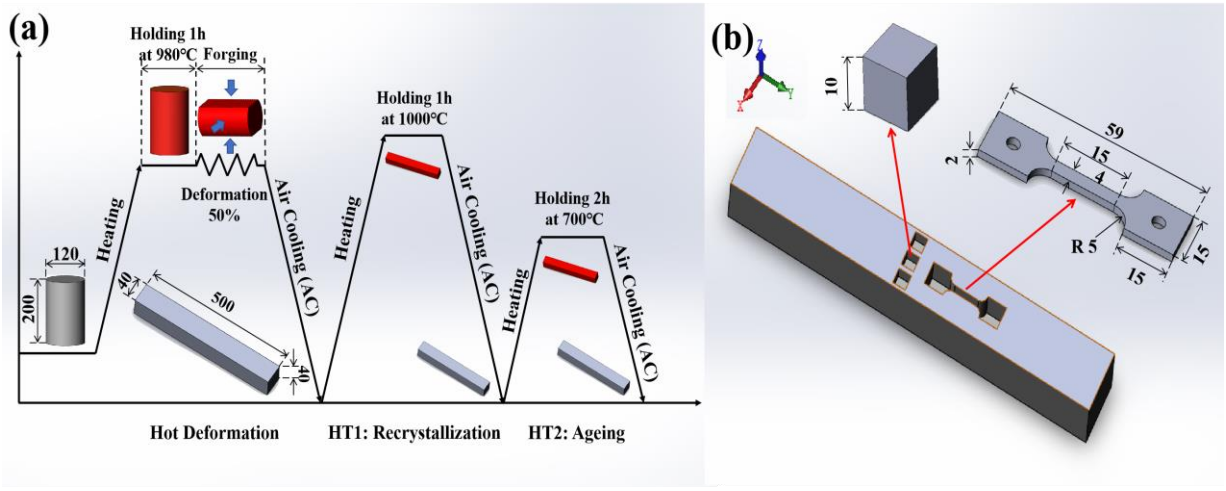

Fig. 2. Schematic of the thermomechanical processing:

(a) Hot working process, (b) Position, geometry and dimensions of specimens (in mm)

2.3. Microstructural observation

X-ray diffraction phase analysis was conducted using a diffractometer (XRD, D-max 2550V), operating at 40 kV and 20 mA with a scanning rate of 5 °/min. The data were collected for a 2θ angle ranging from 20° to 80°. Microstructure investigation was performed on an optical microscope (OM, MEF4A/M, Leica), a transmission electron microscope (TEM, JEM 2100), a scanning electron microscope (SEM, NOVA, NanoSEM 230, FEI) and electron backscatter diffractometer (EBSD). Samples for OM and SEM were cut from the heat-treated composites into the same size of 10mm×10mm×10 mm (Fig. 2(b)) and prepared using conventional grinding and mechanical polishing techniques. The polished samples were etched in HF (AR, vol.%): HNO_3 (aqueous solution): H_2O = 1:3:10. TEM samples were cut from the tensile test specimen and mechanically ground to about 50 μm in thickness, followed by twin-jet electropolishing in a solution of 6% $HClO_4$, 64% CH_3OH and 30% C_4H_9OH (in volume) at -40 ℃ and at a voltage of 35 V to obtain the electron transparent region.

2.4. Tensile test

The specimen design followed previous publications [31,32] and all the tensile specimens were cut with the same dimension of 15 mm×4 mm×2 mm, as shown in Fig. 2(b). Before testing, samples were polished and the thickness was controlled to 1.5mm±0.05mm. Room temperature tensile tests were conducted on ZwickT1 - FR100TN, A50 at a strain rate of $10^{-3}s^{-1}$. High temperature tensile tests were performed on MHIMADZU at 600℃, 650℃, 700℃ and 750℃ and the heating rate of the furnace was 10℃/min. At least two samples were tested for each condition and the average values

were evaluated after the tensile test. The fracture surfaces were observed using SEM, and the phases were identified using EDS.

3. Results

3.1. Phase identification

Fig. 3 shows the X-ray diffraction patterns of all composites. Mainly Ti and TiB were found in each composite and no diffraction peaks of the raw materials were observed, which indicated that the in-situ reactions were carried out thoroughly during the smelting process. However, due to the large solid solubility of C (approximately 0.48 wt.% in α Ti) and the low content of rare earth oxide, almost no peaks of TiC and La_2O_3 were detected. As the volume fraction of the reinforcements increased, the intensity of TiB phase gradually increased, as shown in the XRD patterns (Fig. 3), which indicated the increase of TiB phase. Owing to the lattice distortion caused by the solid solution of B and C in the matrix, the diffraction peaks of Ti had a slight shift.

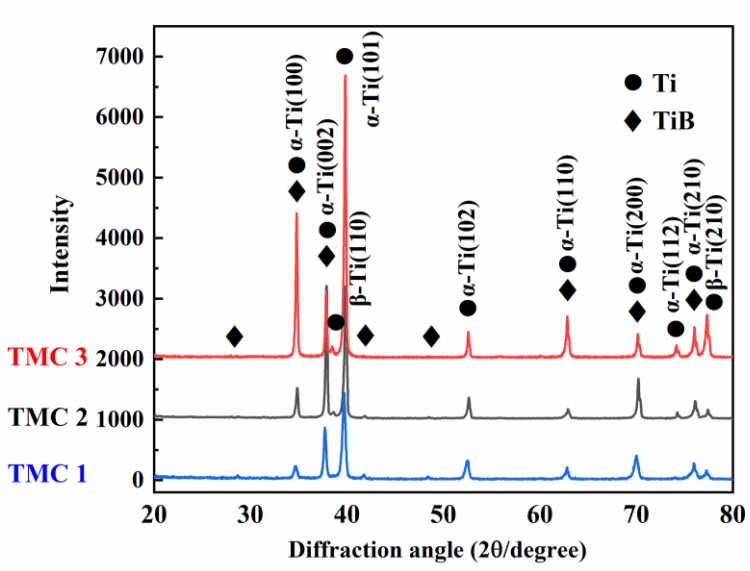

Fig. 3. X-ray diffraction patterns of the heat-treated composites with different reinforcement contents

3.2. Microstructure

Fig. 4 presents the OM micrographs of (TiB+TiC+La_2O_3)/IMI834 composites in both cross section and vertical section after heat treatment. The reinforcements were distributed perpendicular to the forging direction and formed banded reinforcement-rich regions. With the increase of the reinforcement content, the spacing of the reinforcement-rich regions decreased and the matrix microstructure exhibited remarkable difference with clear pattern. As shown in Fig. 4, the

heat-treated TMCs consisted of the primary equiaxed α and transformed lamella α phases. For TMCs 1, the amount of transformed α lamella was approximately 30%. When the reinforcements content increased to 5.0 vol.%, almost no transformed α lamella microstructure were observed and the matrix exhibited complete equiaxed microstructure. This shows that the increase of reinforcement content can lead to the transformation from lamella α grains to equiaxed α grains.

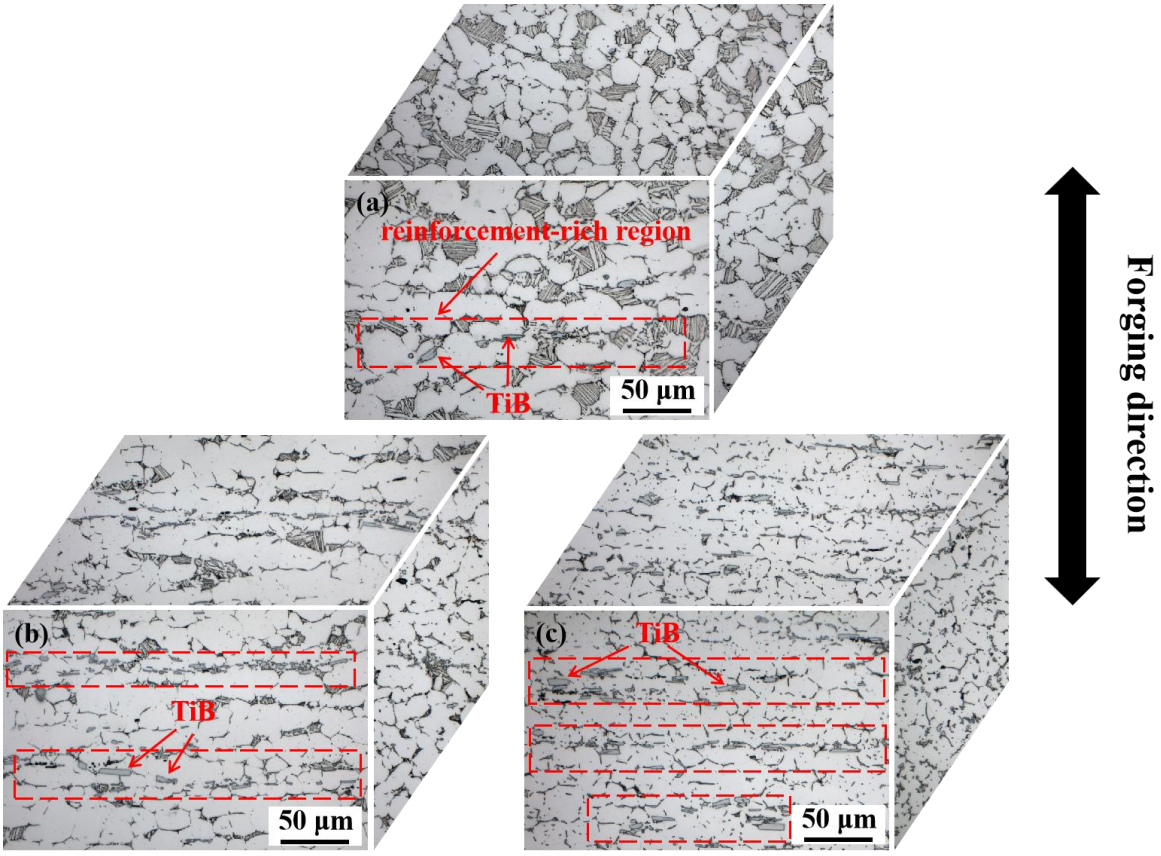

Fig. 4. Optical micrographs of (TiB+TiC+La_2O_3)/IMI834 composites with different reinforcement fractions: (a) 0.5 vol.%, (b) 2.5 vol.%, (c) 5.0 vol.%

To better understand the distribution and composition of reinforcements, SEM, EDS and TEM were used for further analysis of the microstructure. Fig. 5 shows the SEM images of the heat-treated TMCs obtained by backscattered electrons. Table 2 lists the EDS analysis result of TMCs-2 (Fig. 5(e)). In Fig. 5, the gray area represented the matrix of TMCs. For point B, the black whiskers distributed at the equiaxed grain boundary mainly contained titanium and boron elements, the atomic ratio of Ti to B is approximately 1:1, which proved that the black fibrous areas were TiB. As for point C, the coarse white band areas mainly contained lanthanum (La), tin (Sn) and oxygen elements (O), the atomic ratio of La to Sn is approximately 5:3, which indicated that a ternary rare earth oxides were formed due to interaction among the alloying elements Sn, O and the element La during

the melting process. It is worth noting that although the shape of the white precipitated phases in (d-f) may be different, the EDS results (Fig. 5(g~i)) showed that these white phases are similar in chemical composition, which could be identified as the same phase. Although a cluster of La_5Sn_3 and other oxides are present in the composites, the composites are named after the ideally generated reinforced phase La_2O_3, considering the complexity of oxide types and the naming methods of other researches. As for point D, the small white particles dispersed within the equiaxed grain mainly contained titanium (Ti), zirconium (Zr) and silicon elements (Si), combined with the TEM result shown later in Fig. 7(e,f), this kind of particles should be $(TiZr)_5Si_3$ or $(TiZr)_6Si_3$, which is consistent with many silicon-containing titanium alloys [37, 38]. The formation of these nano-scale particles is mainly determined by the composition of matrix-IMI834 alloy.

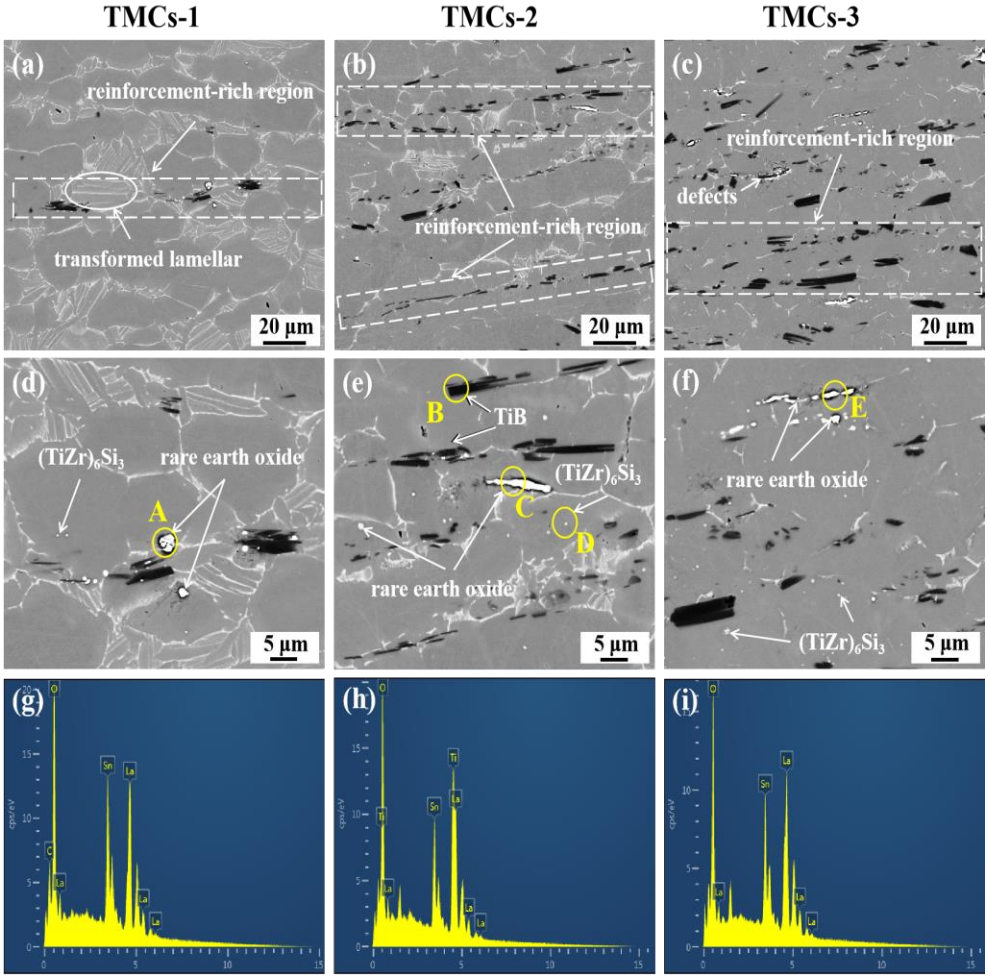

Fig. 5. Backscattered electron SEM micrographs of heat-treated (TiB+TiC+La_2O_3)/IMI834 composites with different reinforcement contents: (a, d) 0.5 vol.%, (b, e) 2.5 vol.%, (c, f) 5 vol.%, (g,h,i) EDS results of the rare earth oxides respectively at position A, C, and E, showing similar chemical composition.

Table 2 EDS results of heat-treated 2.5 vol.% TMCs (Fig. 5(e))

Point	Element	wt.%	at. %
B	Ti	82.7	51.9
	B	17.3	48.1
C	O	25.8	74.1
	La	49.9	16.5
	Sn	24.3	9.4
D	Ti	74.3	79.2
	Zr	20.6	11.5
	Si	5.1	9.3

Based on EDS analysis, almost no TiC particles were detected. Therefore, EBSD was used to further investigate the presence and the distribution of the reinforcements, especially the TiC particles. Fig. 6 shows clear changes in grain size, the morphology and distribution of the reinforcements among samples with different volume fraction of reinforcements. The average grain sizes, measured using image-pro plus, were 21.5μm, 16.7μm and 9.1μm respectively for 0.5, 2.5 and 5.0 vol.% composites, showing better grain refinement with increasing reinforcement contents. The EBSD results indicated that carbons mainly had two existing forms due to the high solid solubility of C: when the theoretical content of TiC was below 1.1 vol.%, the carbon almost completely dissolved in the matrix, as shown in Fig. 6 (a); when the content increased to 2.2 vol.%, the carbon exceeded the solid solubility in the matrix and formed the equiaxed TiC particles, which precipitated at the triple junction, as shown in Fig. 6 (b, c).

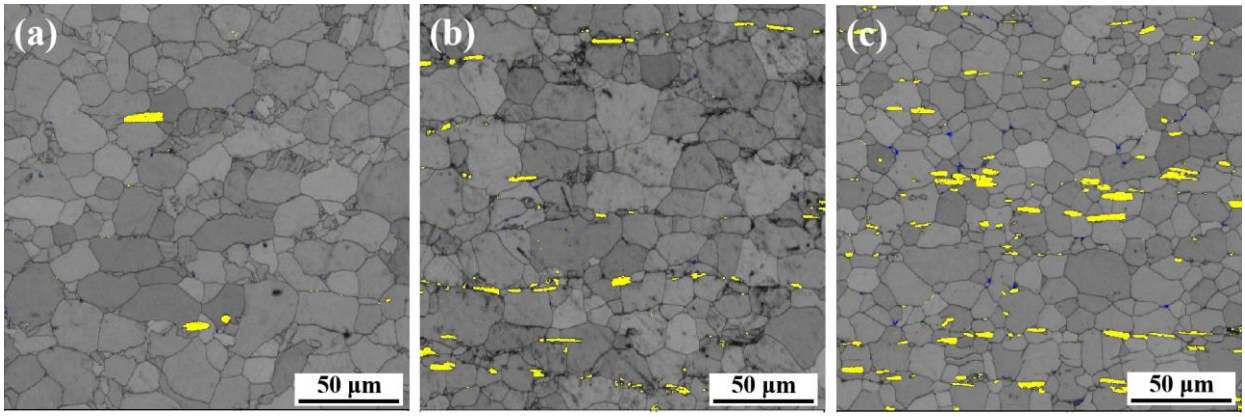

Fig. 6. EBSD results of (TiB+TiC+La_2O_3)/IMI834 composites with different reinforcement content: (a) 0.5 vol.%, (b) 2.5 vol.%, (c) 5.0 vol.%, showing the grain size changes and the distribution of TiC (in blue) and TiB (in yellow).

The SEM micrographs showed micron-scale TiB whiskers and rare earth oxide particles were evenly distributed along the equiaxed α grain boundary and perpendicular to the forging direction, while the nano-scale Ti-Zr-Si particles were distributed inside the equiaxed α grain. Previous researches have shown that TiB whiskers tend to grow along the [010] direction due to the B27 structure [39] and the increase of B content in matrix can promote the growth of TiB and increase the aspect ratio [14]. During forging process, TiB whiskers can rotate and eventually become perpendicular to the forging direction. However, due to the load bearing capacity, the reinforcements, especially the TiB whiskers, induced high stress concentration in the tip region. The large-size TiB whiskers were easily fractured into short fibers during hot forging, resulting in the decrease of the aspect ratio and creating defects. From the study of TC4-based composites [19,20], nano-scale La_2O_3 particles could form with the addition of La in Ti6Al4V matrix. However, different results were observed. Fig. 7 shows the bright-field TEM images of the 2.5 vol.% composites near the fracture regions and the identification of the reinforcements. As shown in Figs. 5 and 7, the element La seemed easy to combine with alloying element Sn and form a micron-scale ternary oxide cluster even at a low content of La. According to [40], La could form intermetallic compounds with Sn like LaSn, La_2Sn_3, La_5Sn_3, etc, while La and Sn could also promote the formation of nano-scale La_2O_3 and SnO_2. From the morphology exhibited in Fig. 7(a,c,d), the rare earth clusters are mainly consisting of the micron-scale rod-like La_5Sn_3 particles with a few nano-scale La_2O_3 and SnO_2 particles around. This kind of clusters had the penetrating crack inside and were easy to create internal defects in the matrix. With the increase of La content, this kind of clusters grew and transformed from globular-like to rod-like during the forging process and created defects at the bonding interface. The results indicated that the La_5Sn_3 particles were very brittle and the bonding between these particles and the matrix interface was weak, so the increase in size of these oxide clusters was not conducive to improve tensile properties. Thus, the formation of these ternary oxide clusters has both positive and negative effect on TMCs, and the addition content of La should be controlled at a low level to optimize the mechanical properties.

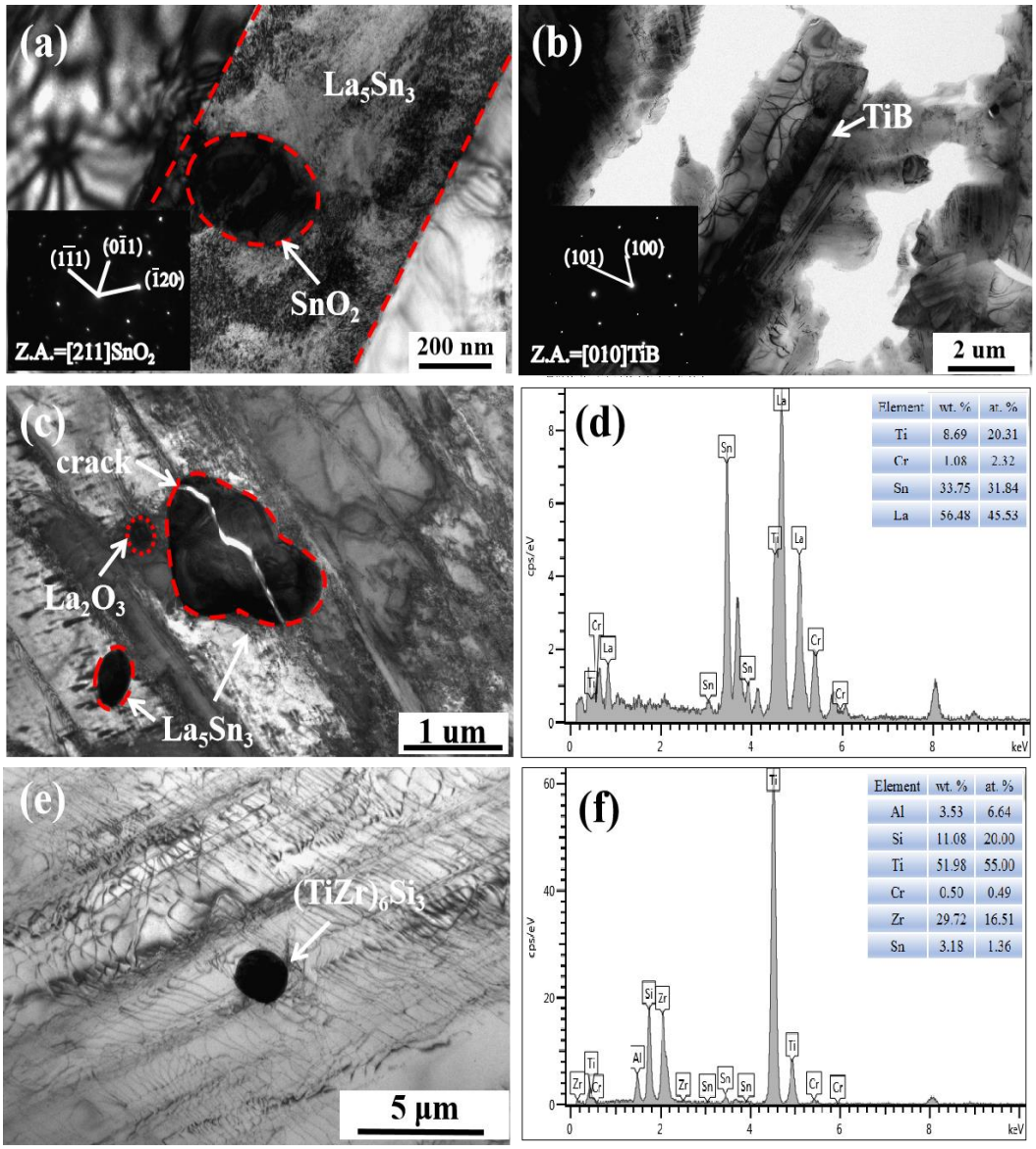

Fig. 7. Bright-field TEM images of 2.5 vol.% (TiB+TiC+La_2O_3)/IMI834 composites near the fracture regions: (a,c,d) Near interface region of the rare earth oxides, (b) Near interface region of TiB, (e,f) Near interface region of $(TiZr)_6Si_3$

3.3. Mechanical Properties

3.3.1. Room temperature tensile properties

Tensile tests at ambient temperature were carried out to investigate the mechanical properties and the strengthening mechanism of the composites. Fig. 8 (a) shows the engineering stress-strain curves of (TiB+TiC+La_2O_3)/IMI834 composites with different reinforcement contents. Obviously, with the increase of reinforcement content, the tensile strength increased while the elongation decreased. As for the TMCs 1, the ultimate strength value was 1118.4 MPa and the elongation was 10.6%, showing a significant improvement over the matrix IMI834 alloy (1030MPa, 6% [41]). Once the

reinforcement content increased to 2.5 vol.%, the ultimate strength was improved to 1214.7 MPa, while the elongation decreased to 5.1%. If the reinforcement content increased further to 5.0 vol.%, the composite exhibited a significant decrease in elongation (only 1.2%) even though the strength reached nearly 1300 MPa, which indicates a typical brittle fracture characteristic. By comparing the present hybrid reinforced IMI834 composites with that of TiB/Ti60 composites [24], binary system ($TiB+La_2O_3$)/IMI834 [32], ternary system ($TiB+TiC+Y_2O_3$)/Ti composites [31] and other high temperature titanium alloy based composites in literature [31, 41, 42], as shown in Fig. 8(c), it can be concluded that hybrid reinforcement and the hot working process play an important role in enhancing the tensile strength of the composites, especially the synergistic strengthening of multi-scale reinforcements.

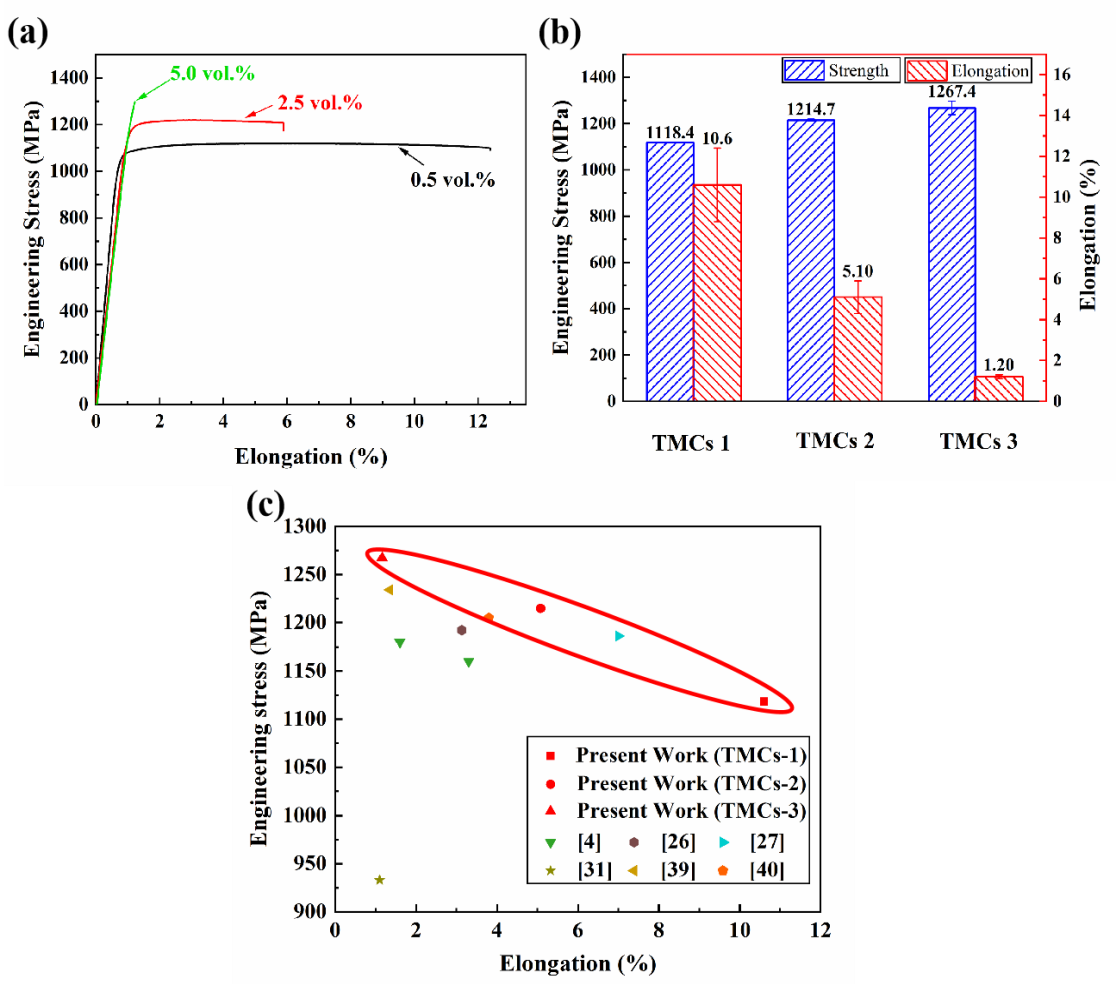

Fig. 8. Engineering stress-strain curves and tensile properties of ($TiB+TiC+La_2O_3$)/IMI834 composites at room temperature: (a) Engineering stress-strain curves, (b) Tensile properties, (c) Comparison of the mechanical properties with other composites, showing the outstanding performance of the TMCs in this study in the red oval.

Fig. 9 shows the tensile fracture surface morphology of (TiB+TiC+La_2O_3)/IMI834 composites at room temperature. Based on the microstructure, the TMCs mainly contained two micron-scale reinforcements: TiB whiskers and ternary oxide clusters, so EDS analysis were used to differentiate TiB and oxide clusters in the fracture. It can be seen that large number of dimples and tearing edges distributed on the fracture surface in the specimen with 0.5 vol.% reinforcement content. The characteristic of the dimple-dominated fracture was consistent with the good elongation. As the reinforcement content increased, the proportion of cleavage section of brittle TiB increased, while the proportion of tearing edges and dimples of ductile matrix decreased. Once the content reached 5.0 vol.%, almost no dimples were observed and the brittle TiB whiskers and the matrix showed obvious characteristics of cleavage fracture, which was consistent with the low elongation (below 2%). This characteristic reflected the variation trend of elongation at room temperature with increasing reinforcement contents.

The variation of the fracture pattern was attributed to the reinforcements, among which TiB whiskers have better loading capacity. From the fracture morphology, no TiB whiskers and oxide particles were pulled out from the matrix, indicating the superior strengthening effect and the strong interface cohesion between the reinforcements and titanium matrix. Meanwhile, previous study showed that cracks would preferentially occur in TiB whiskers and defects during the stretching process [19]. Consequently, the internal cracks formed, the load bearing capacity of TiB whiskers decreased, and the matrix cannot withstand the high stress, which accelerated the fracture, greatly reduced the ductility and even caused the brittle fracture.

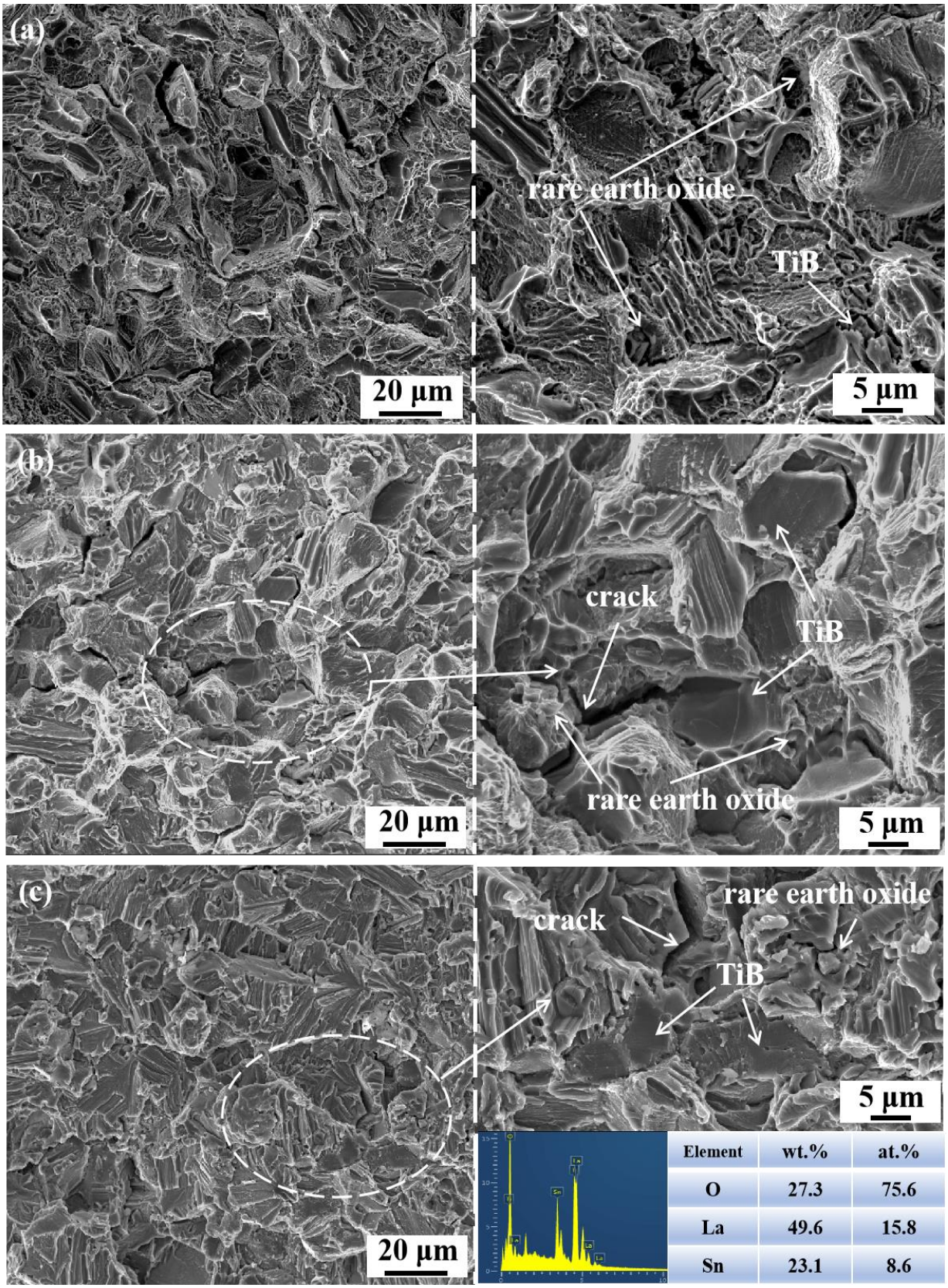

Fig. 9. Fracture morphology of (TiB+TiC+La_2O_3)/IMI834 composites with different reinforcement fractions at room temperature: (a) 0.5 vol.%, (b) 2.5 vol.%, (c) 5.0 vol.%. The insert shows the EDS result of rare earth oxide.

3.3.2. High temperature tensile properties

Similar with high temperature titanium alloy, high temperature strength is one of the main criterions for titanium matrix composites [24]. Fig. 10 shows the high temperature tensile curves of the (TiB+TiC+La_2O_3)/IMI834 composites with different reinforcement contents. Fig. 10(a~c) are nominal engineering strain-stress curves of each TMCs at high temperature. Table 3 listed the tensile properties of the heat-treated (TiB+TiC+La_2O_3)/IMI834 at both room temperature and high temperature. The variation trend of high temperature performance with temperature could be clearly seen in Fig. 10(d~e). As expected, the tensile strength of the composites decreased when the temperature increased from 600℃ to 750℃, and was enhanced when the reinforcement content increased from 0.5 to 5.0 vol.%. For TMCs 2, the tensile strength was increased by 12.6%, 11.9%, 11.7% and 9.3% at 600℃, 650℃, 700℃ and 750℃ compared with TMCs 1, respectively. Furthermore, when the reinforcement content increased to 5.0 vol.%, the tensile strength of TMCs 3 were increased by 32.7%, 26.7%, 19.2% and 20.3% compared with TMCs 1, respectively. It is worth noting that the reinforcement significantly enhanced the strength below 700℃, but when the temperature is above 750℃, the strengthening effect was not evident. Based on the analysis of these test strength values, the high temperature strength was significantly improved by the reinforcements, but the improvement decreased with the increase of temperature.

Table 3. Tensile properties of the thermomechanical processed (TiB+TiC+La_2O_3)/IMI834 composites with different reinforcement contents

T	25 ℃		600 ℃		650 ℃		700 ℃		750 ℃	
Sample	σ_b (MPa)	δ (%)	σ_b (MPa)	δ (%)	σ_b (MPa)	δ (%)	σ_b (MPa)	δ(%)	σ_b (MPa)	δ (%)
TMCs 1	1118.4±0.2	10.6±1.8	643.9	37.3	569.1	58.9	494.7	62.9	375.3	129.8
TMCs 2	1214.7±4.4	5.1±0.8	724.7	34.4	637.9	46.9	552.3	58.1	410.5	104.6
TMCs 3	1267.4±29.9	1.2±0.1	853.4	37.1	721.5	32.8	589.9	43.7	451.1	83.8

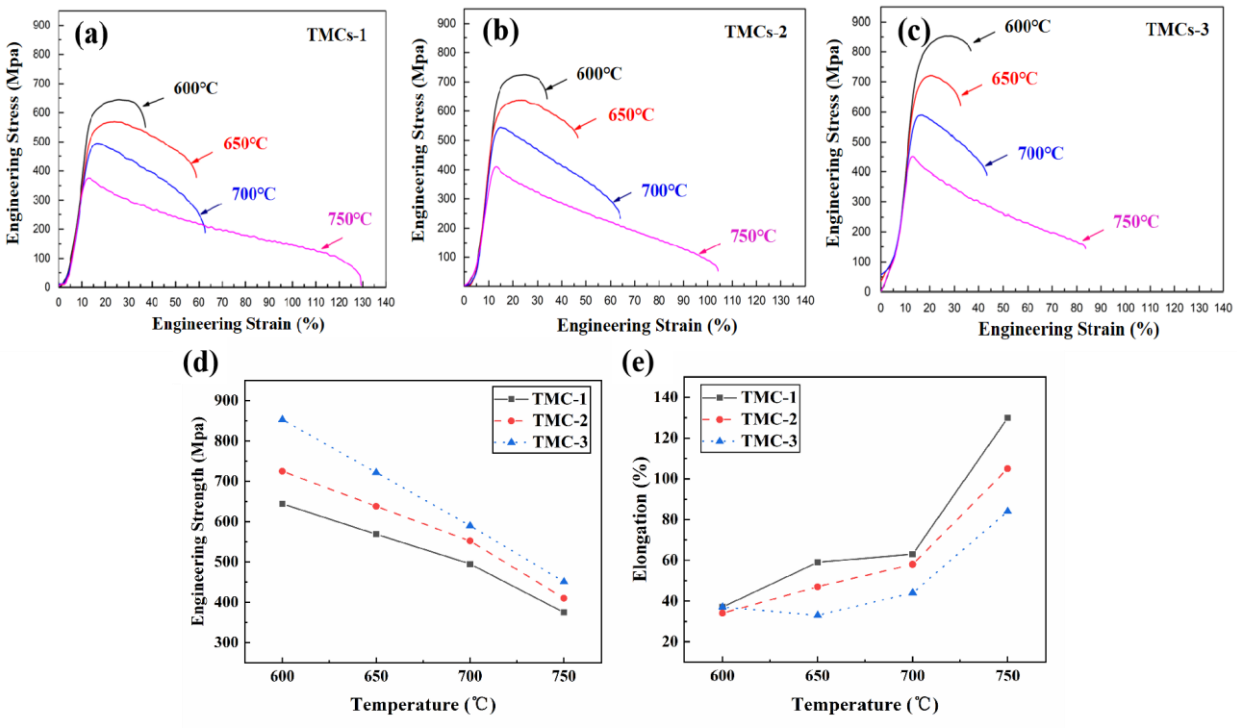

Fig. 10. High temperature tensile curves of (TiB+TiC+La_2O_3)/IMI834 composites with different reinforcement contents: (a) 0.5 vol.%, (b) 2.5 vol.%, (c) 5.0 vol.%, (d) The comparison of high temperature strength, (e) The comparison of high temperature elongation

Fig. 11 shows typical tensile fracture morphology of the 2.5 vol.% (TiB+TiC+La_2O_3)/IMI834 composites at different temperature. Compared with the fracture morphology at room temperature, significant changes were observed at high temperature and large and deep dimples appeared in the morphology which performed obvious ductile fracture characteristics. In addition, the failure types of the reinforcement also changed. It can be observed in Fig. 11 that no whiskers were pulled out from the matrix below 650℃ and the reinforcements failed in the form of fracture, which indicated the interface cohesion between TiB whiskers and matrix was strong enough. However, a few pulled-out TiB whiskers were found when the temperature was raised to 700℃, and almost all the TiB whiskers were pulled out of the matrix at 750℃. The decrease of interfacial bonding strength weakened the resistance effect of the reinforcements to grain slip and, as a result, decreased the strengthening effect of the reinforcements. Thus, the strengthening effect of reinforcement was not obvious over 750℃. From above analysis, the decrease of high temperature strength is mainly caused by two factors, one is the matrix softening, the other is the decrease of interface cohesion between the reinforcements and matrix. From the analysis results of high temperature properties and failure modes, the TMCs fabricated in this study can maintain a good enhancement effect between 650-700℃ and show an

improved high-temperature performance.

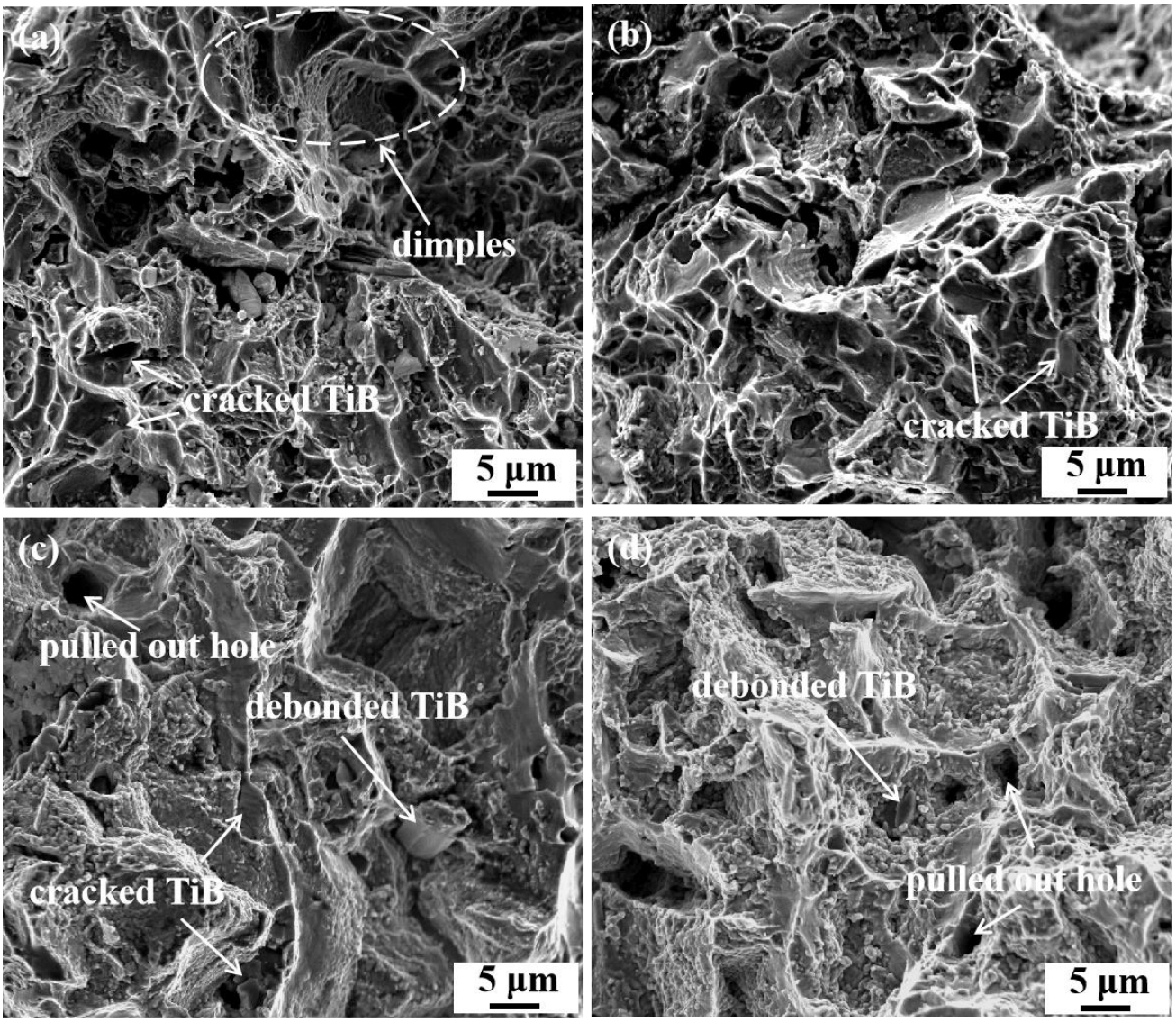

Fig. 11. Fracture morphology of 2.5 vol.% (TiB+TiC+La_2O_3)/IMI834 composites at high temperature: (a) 600℃, (b) 650℃, (c) 700℃, (d) 750℃

4. Discussion

4.1. Microstructural evolution

As observed above, the microstructure of the TMCs showed regular changes. Earlier studies have shown that the reinforcements can stimulate dynamic recrystallization of the matrix during thermal deformation [20, 43]. In this study, the billets were forged in α+β phase region, and dynamic recrystallization and dynamic recovery occurred simultaneously under the combined action of temperature and pressure, forming the deformation microstructure. But the reinforcements,

especially TiB whiskers, have stronger bearing capacity than the matrix and can obstruct dislocation motion during plastic deformation. Thus, compared with reinforcement-lean region, the reinforcement-rich regions stored more energy and provided larger driving force for recrystallization nucleation. Thus, dynamic recrystallization was stimulated and the lamellar grains located at the reinforcement-rich region transformed to the fine equiaxed grains. Moreover, high temperature also provided a good condition for static recrystallization during the subsequent heat treatment process. As a result, further recrystallization occurred and the equiaxed grains also formed in the reinforcement-lean region. Meantime, the primary equiaxed grains grew up. Under the control of thermal deformation and recrystallization heat treatment process, the matrix transformed to a completely fine equiaxed microstructure. The result indicated that the reinforcements can accumulate dislocation and provide driving force for dynamic recrystallization, while the recrystallization heat treatment provided both time and condition for the further static recrystallization. From what has been discussed above, the two recrystallization processes optimized the microstructure under the same deformation: (1) The dynamic recrystallization stimulated by the enhancement of the reinforcement content, (2) The static recrystallization stimulated by the subsequent recrystallization heat treatment. Thus, the adjustment of the hybrid reinforcements content and the heat treatment process successfully optimized the microstructure to obtain a uniform equiaxed microstructure.

To make it more intuitive, a schematic illustration of microstructural evolution of (TiB+TiC+La_2O_3)/TMCs during forging and heat treatment is depicted in Fig. 12, where the typical characteristics of microstructure evolution has been exhibited. As for the matrix, the lamellar grains near the reinforcement-rich region were preferentially transformed to the fine equiaxed grains during forging process due to the dynamic recrystallization stimulated by the reinforcements. Then the reinforcement-lean region transformed into equiaxed grains due to the static recrystallization during the subsequent heat treatment process. As for the reinforcements, the addition element C mainly dissolved into the matrix and acted as solution strengthening rather than the dispersion strengthening at low content. TiB whiskers and rare earth oxide particles were evenly distributed along the equiaxed α grain boundary and perpendicular to the forging direction, which played the role of load strengthening and dispersion strengthening. TiB whiskers were broken into small segments accompanied with micro voids emerging, while the coarse oxide clusters created defects at bonding interface after the forging process. The rare earth oxide particles were transformed from the

globular-like to rod-like during the forging process when penetrating cracks also formed inside the particles at the same time.

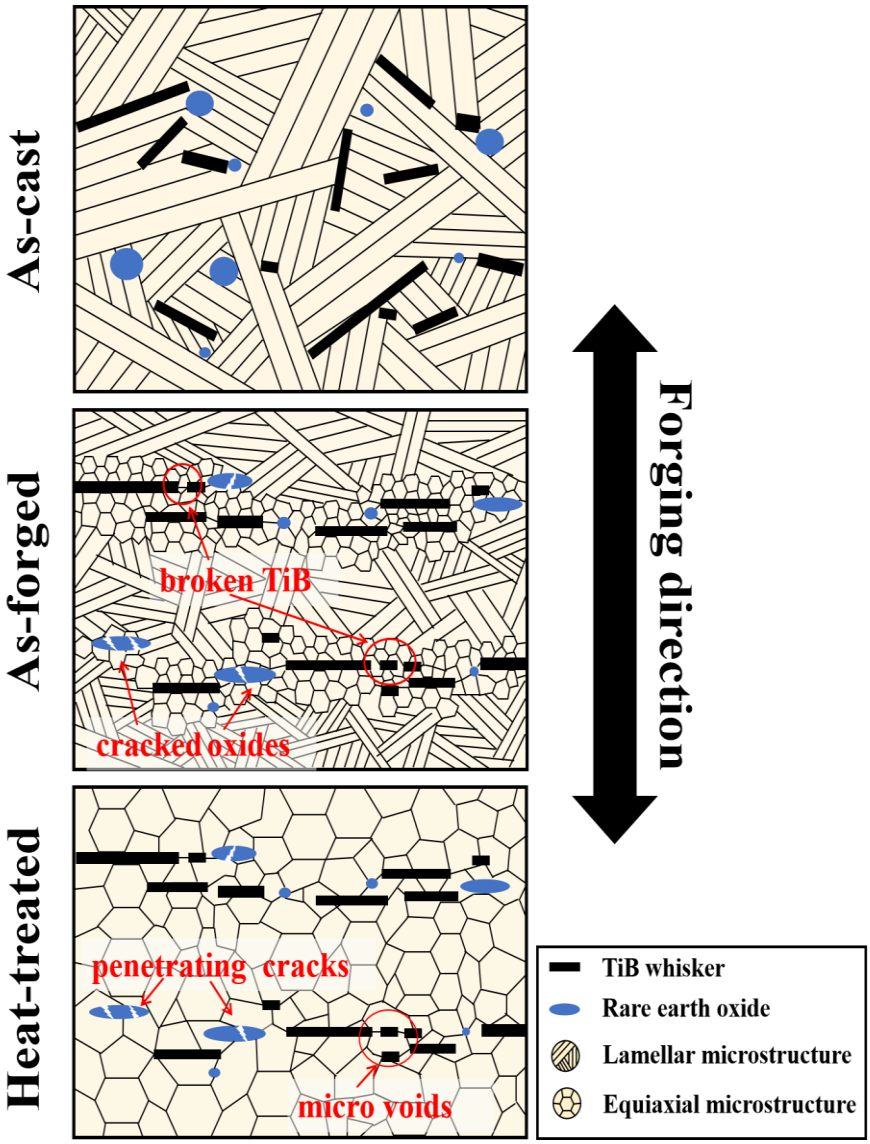

Fig. 12. Schematic of microstructure evolution of the composites during thermomechanical processing

4.2. Synergistic strengthening behavior of hybrid reinforcements

Mechanical properties showed the heat-treated TMCs exhibited excellent performance at both room temperature and high temperature, especially achieving a significant improvement on tensile strength. The improvement could be attributed to the refinement of the matrix grains and the strengthening effect of the ternary reinforcements. The strengthening mechanism was discussed in detail here.

As observed above, the average size of the composites was 21.5μm, 16.7μm and 9.1μm,

respectively, and thus, the hybrid reinforcements successfully reduced the grain size. The refinement could attribute to three factors: (1) The reinforcements hindered the as-cast matrix grain growth during the solidification process, (2) The reinforcements stimulated the dynamic recrystallization and promoted the transformation of lamella α grain to fine equiaxed α grain during the forging process, (3) The reinforcements hindered the primary α grain growth during the heat treatment process, resulting in a reduction in the grain size. According to Hall-Petch slope, the relationship between the strength (σ_m) and the grain size (d_g) can be expressed as:

$$\sigma_{\mathrm{m}} = \sigma_0 + \mathrm{k_m d_g}^{-1/2} \tag{4}$$

where σ_0 is either a frictional stress resisting the motion of gliding dislocations or an internal back stress, k_m is the Hall-Petch slope, which reflects the resistance of grain boundary to slip transfer. The refinement of the grain enhanced the strength of TMCs.

The reinforcement-rich region also played important role in enhancing the TMCs [20-22]. The effect of different reinforcements on tensile strength could also be expressed by the existing model. TiB whiskers mainly played the role of load strengthening. From the bright-field TEM images shown in Fig. 7(b), TiB whiskers obstructed dislocation movement and accumulated high density dislocations tangling around, which further hindered the movement of dislocation. Finally, the TiB whiskers failed in the form of fracture to release the stress. Thus, the TMCs significantly enhanced tensile strength. According to Nardone and Prewo [44] and Yang et al. [34], the strengthening effect of TiB whiskers could be expressed as:

$$\sigma_{\mathrm{cw}} = \sigma_m 0.5 V_w (2 + \frac{l}{d}) + \sigma_m (1 - V_m) \tag{5}$$

where σ_{w} and σ_{m} are the yield stress of the whisker-reinforced TMCs and matrix alloy, V_w is the volume fraction of whiskers, l/d_w is the whisker aspect ratio of length to diameter. Thus, as the volume fraction and the aspect ratio increase, the tensile strength was improved.

There were two existing forms of carbon, the solid solution form at low content and the precipitation form at high content. As the results of SEM and EBSD show, when the theoretical content below 1.1 vol.%, C mainly presented in solid solution form and played the role of solid solution strengthening. The strengthening effect could be expressed by the following formula [45]:

$$\sigma_c = A\frac{x}{a_0^2 b} \quad (6)$$

where A is a constant, x is the atom fraction of carbon, a_0 is the lattice constant of the matrix alloy, b is the Burgers vector. Thus, with the increase of C in solid solution, the strengthening effect was enhanced. In addition, when the theoretical content increased to 2.2 vol.%, carbon was saturated in the matrix and a few TiC particles precipitated along the grain boundary. The small amount TiC played the role of precipitation strengthening. According to Yang et al. [35], the strengthening effect can be expressed by the following formula:

$$\sigma_{cp} = \sigma_m V_p (1 + \frac{(L+t)A_0}{4L}) + \sigma_m (1 - V_p) \quad (7)$$

where σ_{cp} is the yield stress of particle-reinforced TMCs, L is the length of the particle perpendicular to the applied stress and A_0 is the particle aspect ratio. Thus, carbon had two strengthening effects at high content and the TMCs were further enhanced.

Last but not the least, the La element mainly played the role of reducing the oxygen content, the generation of La_2O_3 and ternary oxides can significantly reduce oxygen content. However, these kinds of oxide cluster had little resistance to dislocations. The penetrating cracks revealed that the bearing capacity of the cracked oxide clusters was poor, instead of strengthening, these crack may become a source for accelerated fracture. Thus, the addition element La mainly acted as oxygen absorber to reduce the oxygen contents in matrix and only a small amount of nano-scale La_2O_3 and $(TiZr)_6Si_3$ particles acted as the precipitation-phase to enhance the strength.

In general, the strengthening mechanism of the hybrid-reinforced TMCs mainly attributed to the following aspects: (1) refinement of the matrix α grain size, (2) load strengthening of TiB whiskers, (3) solid solution strengthening of C element and the precipitated-phase strengthening of TiC particles, and (4) reduction of oxygen in the IMI834 matrix.

4.3. Effect of the hybrid reinforcements on the elongation

Contrary to the increase in tensile strength, the elongation at both room temperature and high temperature decreased, especially at high reinforcement content. Based on the matrix microstructure, the elongation of equiaxed grain structure should be higher, however, the present experiments showed the opposite result. The research showed that the reinforcement content and matrix

microstructure had synergistic effect on the elongation. On one hand, when the reinforcement content at a low level (0.5 vol.%), negative effects generated by reinforcements were not obvious. Meanwhile, due to the recrystallization stimulated by reinforcements and heat treatment, many fine equiaxed grains were formed in the reinforcement-rich region, while the lamellar grains located at the reinforcement-lean region were also refined, which led to better elongation. Moreover, the addition of La element effectively reduced the oxygen content and also played an important role in improving the ductility. On the other hand, when the reinforcement content increased to a high level, the reinforcements and defects played a dominant role in reducing the elongation. Firstly, the high content of C in the matrix caused the lattice distortion of the matrix alloy and obstructed the dislocation movement on the slip plane, resulting in lower elongation. Secondly, the fracture of TiB whiskers also created micro voids in the matrix, which created the defects in the bonding interface. Thirdly, the coarse ternary oxide particles caused penetrating defects at the bonding interface and cracks were generated preferentially at the defects and the micro voids under the tensile force and higher stress accumulated at the crack tip, which accelerated the fracture and significantly reduced the elongation of TMCs. Compared with previous researches, it is speculated that the segregation and growth of La, Sn and O clusters was the main reason for the sharp reduction of the elongation. Therefore, the addition of reinforcements can improve the performance of the TMCs, but the content needs to be limited. A better combination of strength and ductility can be obtained due to the synergistic effect of the reinforcements and the microstructure at low reinforcement content (not more than 2.5 vol.%).

5. Conclusions

In the present study, hybrid-reinforced IMI834 titanium matrix composites were successfully fabricated by common casting, followed by forging and two-steps heat treatment to optimize the microstructure and strength of the TMCs. The existing forms of reinforcements, microstructure evolution, strengthening mechanism and mechanical properties at both room and high temperature were investigated in detail. The following conclusions were obtained:

(1) The enhancement of the reinforcement content stimulated the dynamic recrystallization during the forging process, while the subsequent heat treatment stimulated the static recrystallization of the matrix, both of which promoted the transformation from lamellar grains to fine equiaxed

grains.

(2) Rare earth element La reacted with the alloy element Sn and formed the micron-scale cluster of ternary oxides, which significantly reduced the ductility by creating defects in the bonding interface, especially at high content.

(3) The mechanical properties of TMCs was improved obviously when the reinforcement content was limited at a low level (below 2.5 vol.%), the strengthening mechanism could be attributed to the refinement of the matrix grain, the solid solution strengthening of C element and the load bearing of TiC, TiB and ternary oxide clusters.

(4) A well-matched condition between microstructure and mechanical properties was obtained when the reinforcement content is 2.5 vol.%. The tensile strength at room temperature and high temperature (700 °C) was increased to 1214 MPa and 552 MPa, while maintaining a good elongation of 5.1% and 58% respectively.

Acknowledgments

This work was supported by National Nature Science Foundation of China (Grant No: U1602274, 51875349, 51871150, 51821001); National Key R&D Program of China (2018YFB1106403); Shanghai Science and Technology Committee Innovation Grant (17JC1402600, 17DZ1120000); Major Special Science and Technology Project of Yunnan Province (NO. 2018ZE002); the Equipment Pre-Research Foundation (41422010509, 61409230409); the 111 Project (Grant No. B16032); and the financial support from China Scholar Council (CSC) (No 201806235029).

Data Availability

The raw data required to reproduce these findings are available upon request by email to the corresponding author: hyuf1@sjtu.edu.cn

References

[1] S.C. Tjong, Y.W. Mai, Processing-structure-property aspects of particulate-and whisker-reinforced titanium matrix composites[J]. Composites Science and Technology, 2008, 68(3-4):583-601.

[2] K. Morsi, V.V. Patel, Processing and properties of titanium–titanium boride (TiBw) matrix

composites—a review[J]. Journal of Materials Science, 2007, 42(6):2037-2047.

[3] K.S.R. Chandran, K.B. Panda, S.S. Sahay, TiBw-reinforced Ti composites: processing, properties, application prospects and research needs[J]. JOM, 2004, 56(5):42-48.

[4] H.Y. Lu, D.L. Zhang, B. Gabbitas, et al. Synthesis of a TiBw/Ti6Al4V composite by powder compact extrusion using a blended powder mixture[J]. Journal of Alloys and Compounds, 2014, 606:262-268.

[5] Y.B. Liu, Y. Liu, H.P. Tang, et al. Fabrication and mechanical properties of in situ TiC/Ti metal matrix composites[J]. Journal of Alloys and Compounds, 2011, 509:3592-3601.

[6] C. Suryanarayana, Mechanical alloying and milling[J]. Progress in Materials Science, 2001, 46(1-2):1-184.

[7] M.A. Lagos, I. Agote, G. Atxaga, O. Adarraga, et al. Fabrication and characterisation of titanium matrix composites obtained using a combination of self propagating high temperature synthesis and spark plasma sintering[J]. Materials Science and Engineering A, 2015:655 44-49.

[8] Z.Y. Fu, H. Wang, W.M. Wang, et al. fabricated by selfpropagating high-temperature synthesis[J]. Journal of Materials Processing Technology, 2003, 137(1-3):30-34.

[9] Z.H. Zhang, X.B. Shen, S. Wen, et al. In situ reaction synthesis of Ti-TiB composites containing high volume fraction of TiB by spark plasma sintering process[J]. Journal of Alloys and Compounds, 2010, 503(1):0-150.

[10] S.G. Tabrizi, S.A. Sajjadi, A. Babakhani, et al. Influence of spark plasma sintering and subsequent hot rolling on microstructure and flexural behavior of in-situ TiB and TiC reinforced Ti6Al4V composite[J]. Materials Science and Engineering A, 2015, 624(29):271-278.

[11] X.N. Zhang, W.J. Lu, D. Zhang, et al. In situ technique for synthesizing (TiB + TiC)/Ti composites[J]. Scripta Materialia, 1999, 41(1):39-46.

[12] V.K. Chandravnshi, R. Sarkar, S.V. Kamat, T.K. Nandy, et al. Effect of boron on microstructure and mechanical properties of thermomechanically processed near alpha titanium alloy Ti-1100[J]. Journal of Alloys and Compounds, 2011, 509(18):0-5514.

[13] W.J. Lu, D Zhang, X.N. Zhang, et al. Microstructural characterization of TiC in in situ synthesized titanium matrix composites prepared by common casting technique[J]. Journal of Alloys and Compounds, 2001, 327:248-252.

[14] Ranganath S . A Review on Particulate-Reinforced Titanium Matrix Composites[J]. Journal of

Materials Science, 1997, 32(1):1-16..

[15] R.A. Gaisin, V.M. Imayev, R.M. Imayev, et al. Effect of hot forging on microstructure and mechanical properties of near α titanium alloy/TiB composites produced by casting[J]. Journal of Alloys and Compounds, 2017, 723:385-394.

[16] L.J. Huang, L. Geng, B. Wang, et al. Effects of hot extrusion and heat treatment on the microstructure and tensile properties of TiB_W/Ti6Al4V composites with a novel network microstructure[J]. Composites Part A : Applied Science & Manufacturing, 2012, 43(3):486–491.

[17] G.F. Huang, X.L. Guo, Y.F. Han, L.Q. Wang, et al. Effect of extrusion dies angle on the microstructure and properties of (TiB + TiC)/Ti6Al4V in situ titanium matrix composite[J]. Materials Science and Engineering A, 667:317–325.

[18] C.J. Zhang, X. Li, S.Z. Zhang, et al. Effects of direct rolling deformation on the microstructure and tensile properties of the 2.5 vol % (TiBw + TiCp)/Ti composites[J]. Materials Science and Engineering A, 2017, 684:645–651.

[19] J. Xiang, Y.F. Han, J.W. Le, et al. Effect of temperature on microstructure and mechanical properties of ECAPed (TiB + La_2O_3)/Ti-6Al-4V composites[J]. Materials Characterization, 2018, 146:149-158.

[20] P.K. Qiu, H. Li, X.L. Sun, et al. Reinforcements stimulated dynamic recrystallization behavior and tensile properties of extruded (TiBw + TiCp + La_2O_3)/ Ti6Al4V composites[J]. Journal of Alloys and Compounds, 2017, 699:874-881.

[21] L.J. Huang L J, L Geng, H.Y. Xu, et al. In situ TiC particles reinforced Ti6Al4V matrix composite with a network reinforcement architecture[J]. Materials Science and Engineering A, 2011, 528(6):2859-2862.

[22] L.J. Huang, L. Geng, H.X. Peng,et al. Room temperature tensile fracture characteristics of in situ TiBw/Ti6Al4V composites with a quasi-continuous network architecture[J]. Scripta Materialia, 2011, 64(9):844-847.

[23] L.J. Huang, L. Geng, A.B. Li, et al. In situ TiBw/Ti-6Al-4V composites with novel reinforcement architecture fabricated by reaction hot pressing[J]. Scripta Materialia, 2009, 60:996–999.

[24] L.J. Huang, F.Y. Yang, H.T. Hu, et al. TiB whiskers reinforced high temperature titanium Ti60 alloy composites with novel network microstructure[J]. Materials and Design, 2013, 51:421-426.

[25] M.Y. Koo, J.S. Park, M.K. Park, et al. Effect of aspect ratios of in situ formed TiB whiskers on the mechanical properties of TiBw/Ti-6Al-4V composites[J]. Scripta Materialia, 2012, 66(7):487-490.

[26] S.D. Luo, Self-assembled, aligned TiC nanoplatelet-reinforced titanium composites with outstanding compressive properties[J]. Scripta Materialia, 2013, 69(1):29-32.

[27] Z.Y. Ma, R.S. Mishra, S.C. Tjong, et al. High-temperature creep behavior of TiC particulate reinforced Ti-6Al-4V alloy composite[J]. Acta Materialia, 2002, 50(17):4293-4302.

[28] J.H. Yang, S.L. Xiao, Y.Y Chen, et al. Effects of nano-Y_2O_3 addition on the microstructure evolution and tensile properties of a near-α titanium alloy[J]. Materials ence and Engineering, 2019, 761(JUL.22):137977.1-137977.9.

[29] X.L. Guo, L.Q. Wang, J.N. Qin, et al. Microstructure and mechanical properties of (TiB + La_2O_3)/Ti composites heat treated at different temperatures[J]. Transactions of Nonferrous Metals Society of China, 2014.

[30] R.W. Bush, C.A. Brice, Elevated temperature characterization of electron beam freeform fabricated Ti-6Al-4V and dispersion strengthened Ti-8Al-1Er[J]. Materials Science and Engineering A, 2012, 554:12–21.

[31] X.L Guo, L.Q. Wang, M.M Wang, et al. Effects of degree of deformation on the microstructure, mechanical properties and texture of hybrid-reinforced titanium matrix composites[J]. Acta Materialia, 2012, 60(6-7):2656-2667.

[32] J.X. Li, L.Q. Wang, J.N. Qin, et al. Effect of microstructure on high temperature properties of in situ synthesized (TiB + La_2O_3)/Ti composite[J]. Materials Characterization, 2012, 66:93-98.

[33] J.H. Yang, S.L. Xiao, Y.Y Chen, et al. The tensile and fracture toughness properties of a (TiBw + TiCp)/Ti–3.5Al–5Mo–6V–3Cr–2Sn–0.5Fe composites after heat treatment[J]. Materials Sience and Engineering: A, 2018, 729:21-28.

[34] Z.F. Yang, W.J. Lu, J.N. Qin, et al. Microstructure and tensile properties of in situ synthesized (TiC + TiB + Nd_2O_3)/Ti-alloy composites at elevated temperature[J]. Materials Science and Engineering A, 2006, 425:185–191.

[35] Z.F. Yang, W.J. Lu, L. Zhao, et al. Microstructure and mechanical property of in situ synthesized multiple-reinforced (TiB + TiC + La_2O_3)/Ti composites[J]. Journal of Alloys and Compounds, 2008, 455(1-2):0-214.

[36] J.H. Yang, Y.Y. Chen, S.L. Xiao, et al. Effect of reinforcements on β→α transformation and tensile properties of a near α titanium matrix composite[J]. Materials Science and Engineering A, 2019, 766:138337.

[37] S. Tkachenko, O. Datskevich, L. Kulak, S. Jacobson, et al. Wear and friction properties of experimental Ti–Si–Zr alloys for biomedical applications[J]. Journal of the Mechanical Behavior of Biomedical Materials, 2014, 39:61-72.

[38] B. Wang, L.J. Huang, L. Geng, et al. Effects of heat treatments on microstructure and tensile properties of as-extruded TiBw/near-α Ti composites[J]. Materials and Design, 2015, 85(Nov.15):679-686.

[39] W.J. Lu, D. Zhang, X.L. Zhang, et al. HREM study of TiB/Ti interfaces in a TiB-TiC in situ composite[J]. Scripta Materialia, 2001, 44(7):1069-1075.

[40] X. Chen, Y.H. Zhuang, Y.G. Chen, et al. Investigation on the 773 K isothermal section of La-Fe-Sn ternary systems by X-ray powder diffraction[J]. Rare Metals, 2010, 29:567-571.

[41] W.J. Lu, D. Zhang, X.N. Zhang, et al. Microstructure and tensile properties of in situ (TiB + TiC)/Ti6242 (TiB : TiC=1:1) composites prepared by common casting technique[J]. Materials Science and Engineering A, 2001, 311(1-2):142-150.

[42] Y.F. Han, J.X. Li, G.F. Huang, et al. Effect of ECAP numbers on microstructure and properties of titanium matrix composite[J]. Materials and design, 2015, 75:113-119.

[43] P.W. Liu, Y.F. Han, P.K. Qiu, et al. Isothermal deformation and spheroidization mechanism of (TiB + La_2O_3)/Ti composites with different initial structures[J]. Materials Characterization, 2018, 146:15-24.

[44] V.C. Nardone, K.M. Prewo. On the strength of disloction of discontinuous silicon-carbide reinfoced aluminum composites[J]. Scripta Metallurgica, 1986, 20(1):0-48.

[45] H. Somekawa, Y. Osawa, T. Mukai, et.al. Effect of solid-solution strengthening on fracture toughness in extruded Mg–Zn alloys[J]. Scripta Materialia, 2006, 55(7):593-596.